Supplementary Materials

High-efficient elimination of spiramycin by Fe_3O_4/ZSM-5/Sch via heterogeneous photo-Fenton oxidation at neutral pH

Jiali Yi[1], Junjun Xu[1,*], Jiatong Liu[1], Yue Zheng[2] and Qiong Wang[1]

[1] College of Chemistry and Materials Engineering, Bohai University, Jinzhou 121013, China

[2] School of Chemistry and Environmental Engineering, Liaoning University of Technology, Jinzhou 12100, China

---

* Correspondence: xujunjun@bhu.edu.cn; Tel.: +86-152-4164-3885

1. Experimental

1.1 Chemicals and reagents

Hydrogen peroxide (H_2O_2, 30 wt.%), perchloric acid ($HClO_4$, ≥ 98 vol.%), sulfuric acid (H_2SO_4, ≥98 vol.%), sodium hydroxide (NaOH, ≥96%), spiramycin (SPM, ≥90%), ferrous sulfate ($FeSO_4·7H_2O$, ≥99%), 1,10-phenanthroline hydrate ($C_{12}H_8N_2·H_2O$, ≥99%), hydroxylamine hydrochloride ($NH_2OH·HCl$, ≥98.5%), methanol (CH_3OH, ≥99%), silver nitrate ($AgNO_3$, ≥98.5%), potassium iodide (KI, ≥99%), sodium sulfate (Na_2SO_4, ≥98.5%), tert-butanol ($C_4H_{10}O$, ≥98.5%) and benzoquinone (BQ, ≥99%) were purchased from Aladdin Chemistry Co., China. Zeolite Socony Mobil-5 (ZSM-5) was provided by Tianjin Yuanli Chemical Co., China.

1.2 Analytical methods

Powder X-ray diffraction (XRD, Rigaku Rotaflex D/max, Japan) was recorded by an XRD-Rigaku Rotaflex D/max diffractometer with Ni-filtered Cu $K\alpha$ radiation (λ=1.541 Å) and a scintillator detector (40 kV, 40 mA) at room temperature with a step speed of 5 deg/min and a scan range from 10^o to 80^o. FTIR spectra were measured on an FEI-Quanta 400 FEG spectrometer (USA) in KBr pellets. The specific conditions were a wave number scan range of 400-4000 cm^{-1}, a resolution of 2.000 cm^{-1} and a scan number of 32. The microstructure images of catalysts (50 mg) were observed by Scanning electron microscopy (SEM, FEI Quanta 400 FEG, 10 kV, USA) and transmission electron microscopy (TEM, FEI-Tecnai G^2 F20, 200 kV, USA). SEM testing required a small amount of the sample to be applied to the conductive adhesive, which was plated to enhance its conductivity before being fixed on the sample stage for characterization, while TEM

testing required a small amount of the sample to be ultrasonically dispersed in anhydrous ethanol; then, a small amount of the suspension was removed and dropped onto a carbon-coated copper grid, and the sample was allowed to dry naturally before testing. High-resolution TEM (HRTEM) and energy dispersive spectroscopy (EDS) were performed on the instrument operated at 200 kV. N_2 sorption analysis was performed on a TriStar II 3020 surface area and pore size analyzer (Macmillan, USA) operated at 77 K. The specific area was calculated based on the Brunauer–Emmett–Teller (BET) method. X-ray photoelectron spectrometry (XPS) was conducted using an ESCALAB 250 XI (Thermo Fisher, USA) with an Al Kα line as an excitation source. Adventitious carbon (248.8 eV) was used as a reference to calibrate the binding energy. UV–vis diffuse reflectance spectra (DRS) were collected on a Cary 100 UV–vis spectrophotometer (Agilent, USA) in the range of 200 nm to 800 nm. The photoluminescence (PL) spectra of the catalysts were measured using a fluorescence spectrometer (FLS980, Edinburgh, UK). A small amount of the sample was compacted on a special carrier sheet, and the excitation wavelength of the sample was set according to the maximum wavelength value measured by UV–visible diffuse reflectance. Electrochemical impedance spectroscopy (EIS), cyclic voltammetry (CV) and the transient photocurrent–time curves (I-t curves) were performed on a CHI 660E electrochemical workstation (Shanghai Chenhua Instrument Co., Ltd., China). The counter, reference and working electrodes were platinum auxiliary electrode, saturated calomel reference electrode (SCE) and glassy carbon disk electrode (GCE), respectively. EIS was measured at an open circuit potential (1 - 10^4 Hz) with an amplitude of 10 mV, and CV was determined at a scan range of 0.3–1.0 V. I-t curves used a 35 W xenon lamp as the visible light source, with a light intensity of 67 $mW \cdot cm^{-2}$. A 0.1 M Na_2SO_4 solution

was employed as the electrolyte. The involved active radicals were analyzed on a Bruker EMX-10/12 (Bruker, Germany) using electron paramagnetic resonance (EPR) with 5,5-dimethyl-1-pyrroline N-oxide (DMPO) (≥97.0%, Aladdin) as a trapping agent. The test conditions were a magnetic field center position (CF) of 3510 G, a scan width (SW) of 100 G, a microwave frequency (MF) of 9.854 GHz, and a power (MP) of 19.82 mW. DMPO was then added by direct addition to the system, and samples were taken directly from the system after 5 min of reaction. Dissolved iron was determined using the 1,10-phenanthroline method [1]. The concentration of target pollution and the amount of total organic carbon (TOC, Vario TOC analyzer) were measured at predefined time intervals. The sample to be measured needs to be filtered through a 0.45 μm filter membrane and then diluted to 10 mL before being tested on the machine.

Degradation intermediates of spiramycin were determined by liquid chromatography–mass spectrometry (LC-MS, TSQ QUANTUM ACCESS MAX, Thermo Scientific, USA). A column (ZORBAX SB-C18, Agilent, USA) was eluted with isocratic solvent for 30 min before it was used. The column temperature was kept at 25℃ during the runs. The mobile phase was a mixture of 0.2 vol.% formic acid aqueous solution and methanol solution (7:3, v/v), and the flow rate was 1 mL/min. The detector wavelength is 232 nm, and the sample should be filtered by a 0.22 μm filter membrane with an injection volume of 20 μL. The negative ion mode was used in the ESI-MS analysis.

1.3 Calculation method

The degradation efficiency (η) was calculated by the following equation (S1):

$$\eta = (C_0 - C_t) / C_0) \times 100\ \% \qquad \text{(S1)}$$

where C_0 is the initial concentration of SPM and C_t is the concentration of SPM at degradation time t (min).

A pseudo first-order kinetic model was used to fit the SPM degradation efficiency equation by the following equation (S2):

$$-\ln (C_t / C_0) = k \cdot t \quad \text{(S2)}$$

where C_0 is the initial concentration of SPM, C_t is the concentration of SPM at degradation time t (min) and k is the apparent first-order kinetics rate (min^{-1}).

The conduction band (CB) and valence band (VB) energies were calculated by the following equation (S3)–(S4):

$$E(CB) = X - E^e - 0.5E_g \quad \text{(S3)}$$

$$E(VB) = E(CB) + E_g \quad \text{(S4)}$$

where E(CB) is the conduction band edge of a semiconductor at the point of zero charges, E(VB) is the valence band edge of a semiconductor, X is the absolute electronegativity of the semiconductor, expressed as the geometric mean of the absolute electronegativity of the constituent atoms, E^e is the energy of free electrons of the hydrogen scale (4.5 eV) and E_g is the band gap energy of the semiconductor.

The contribution percentage (η) of ·OH, $\cdot O_2^-$, h^+, e^- and $SO_4^{\cdot-}$ in the degradation reaction was calculated by the following equation (S6) - (S10):

$$\eta_1 = [(k_{control} - k_{Terbutanol}) / k_{control}] \times 100\ \% \quad \text{(S6)}$$

$$\eta_2 = [(k_{control} - k_{BQ}) / k_{control}] \times 100\ \% \quad \text{(S7)}$$

$$\eta_3 = [(k_{control} - k_{KI}) / k_{control}] \times 100\ \% \quad \text{(S8)}$$

$$\eta_4 = [(k_{control} - k_{AgNO3}) / k_{control}] \times 100\ \% \quad \text{(S9)}$$

$$\eta_5 = [(k_{control} - k_{Methanol}) / k_{control}] \times 100\% - \eta_1 \quad \text{(S10)}$$

Where η_1, η_2, η_3, η_4 and η_5 are the contribution percentages of ·OH, $\cdot O_2^-$, h^+, e^- and $SO_4^{\cdot-}$, respectively.

2. Results and discussion

2.1 Characterization of catalysts

Table S1 Specific surface area, pore volume and pore size of various catalysts

Catalyst	S_{BET} (m^2/g)	Pore volume (cm^3/g)	Pore size (nm)
Fe_3O_4	6.17	0.05	15.68
ZSM-5	253.41	0.16	2.54
Sch	20.04	0.04	8.06
Fe_3O_4/ZSM-5/Sch	205.59	0.15	3.02

2.2 Exploration of reaction conditions

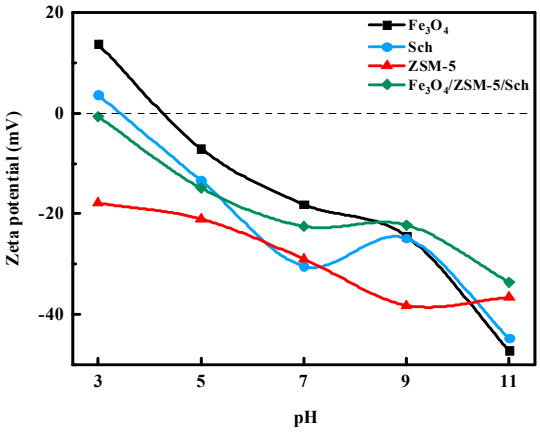

Figure S1 Zeta potential of Fe_3O_4, ZSM-5, Sch and Fe_3O_4/ZSM-5/Sch.

2.3 Identification of active species

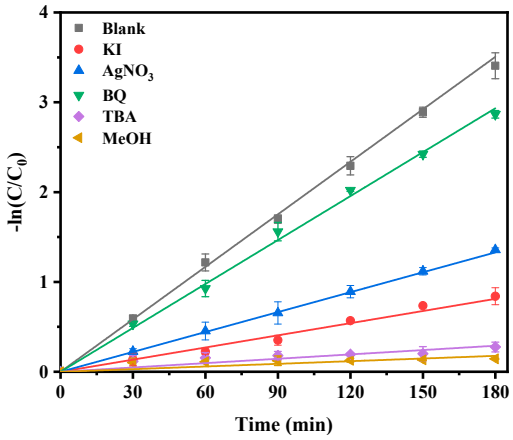

Figure S2 Effect of various radical scavengers on SPM degradation kinetics

Table S2 Pseudo first-order rate constant for the effect of radical quenching agents

Radical quenching agents	Pseudo first-order rate constant (min^{-1})
Black	0.01948
KI	0.00451
$AgNO_3$	0.00738
BQ	0.01630
TBA	0.00161
MeOH	0.00099

2.4 Homogenous photo-Fenton reaction

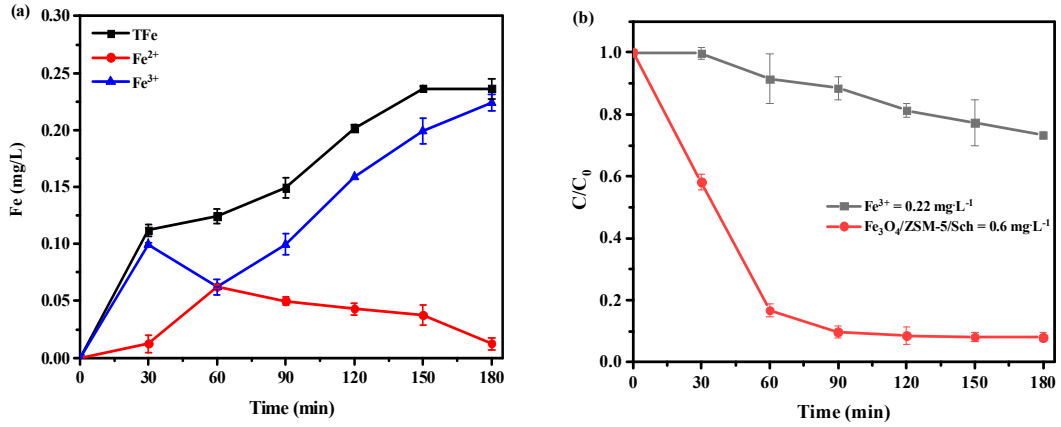

Figure S3 (a) Changes in total Fe-ion (TFe), Fe^{2+} and Fe^{3+} concentration in the UV/Fe_3O_4/ZSM-5/Sch-H_2O_2 system. (b) Comparison of homogeneous and heterogeneous photo-Fenton.

2.5 Enhanced mechanism for catalytic activity

Table S3 Binding energy of iron ions on the surface of Fe_3O_4/ZSM-5/Sch before and after the reaction

	Binding Energy (eV)				**Concentration (%)**	
	Fe^{2+}		Fe^{3+}		≡Fe^{2+}	≡Fe^{3+}
	$2p_{1/2}$	$2p_{3/2}$	$2p_{1/2}$	$2p_{3/2}$		
before reaction	724.17	710.89	727.66	712.87	33.35	66.65
after reaction	723.99	711.69	725.97	713.01	55.64	44.36

2.6 The identification of SPM degradation intermediates

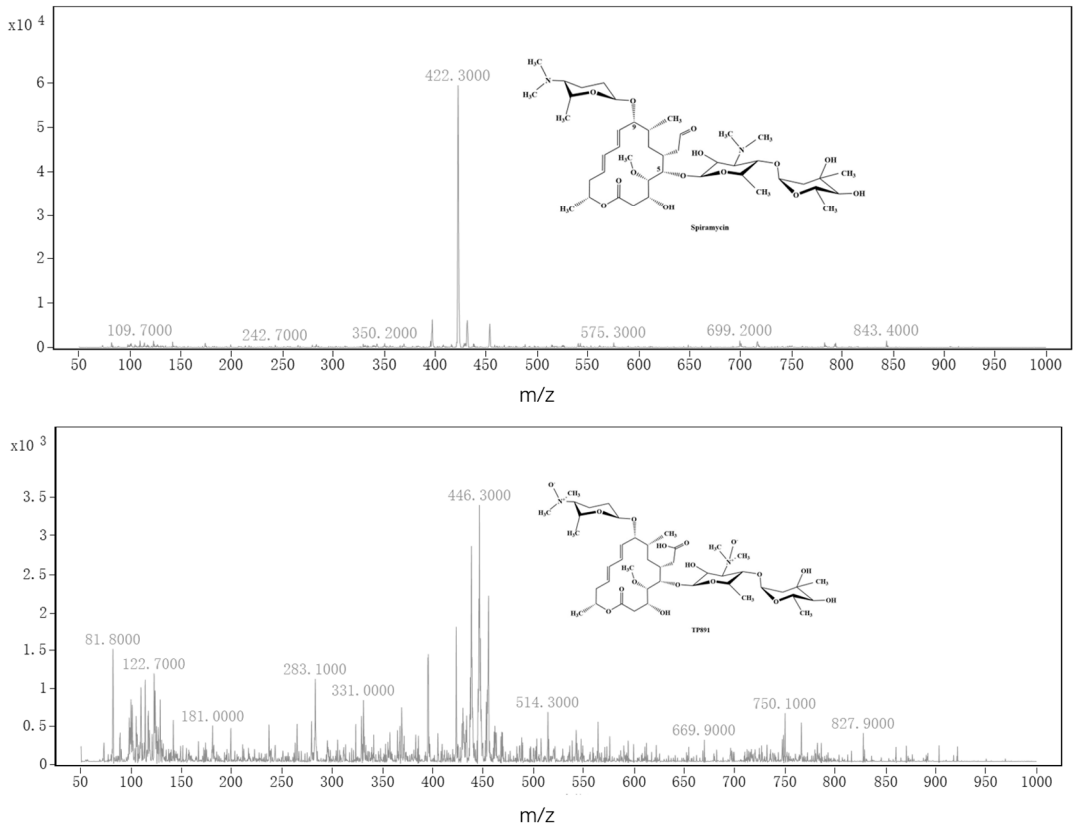

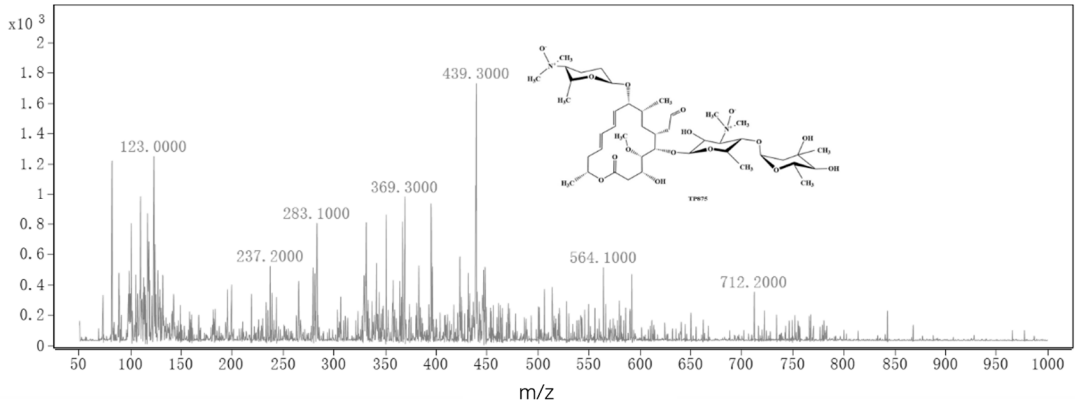
x10 3
439.3000
123.0000
369.3000
283.1000
237.2000
564.1000
712.2000
m/z

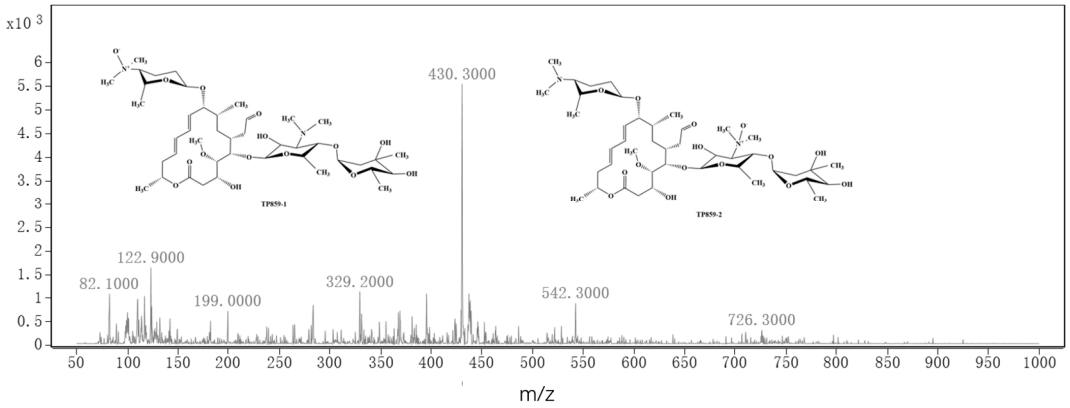
x10 3
430.3000
122.9000
82.1000
199.0000
329.2000
542.3000
726.3000
m/z

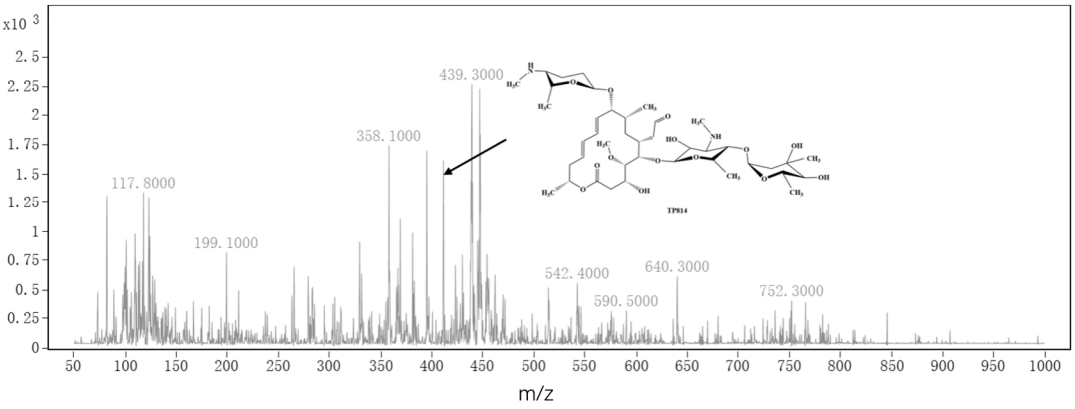
x10 3
439.3000
358.1000
117.8000
199.1000
542.4000
640.3000
590.5000
752.3000
m/z

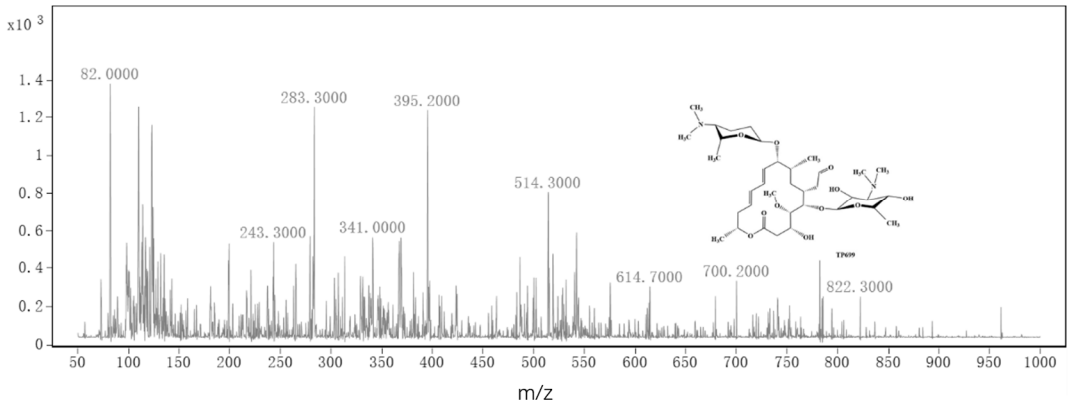
x10 3
82.0000
283.3000
395.2000
514.3000
243.3000
341.0000
614.7000
700.2000
822.3000
m/z

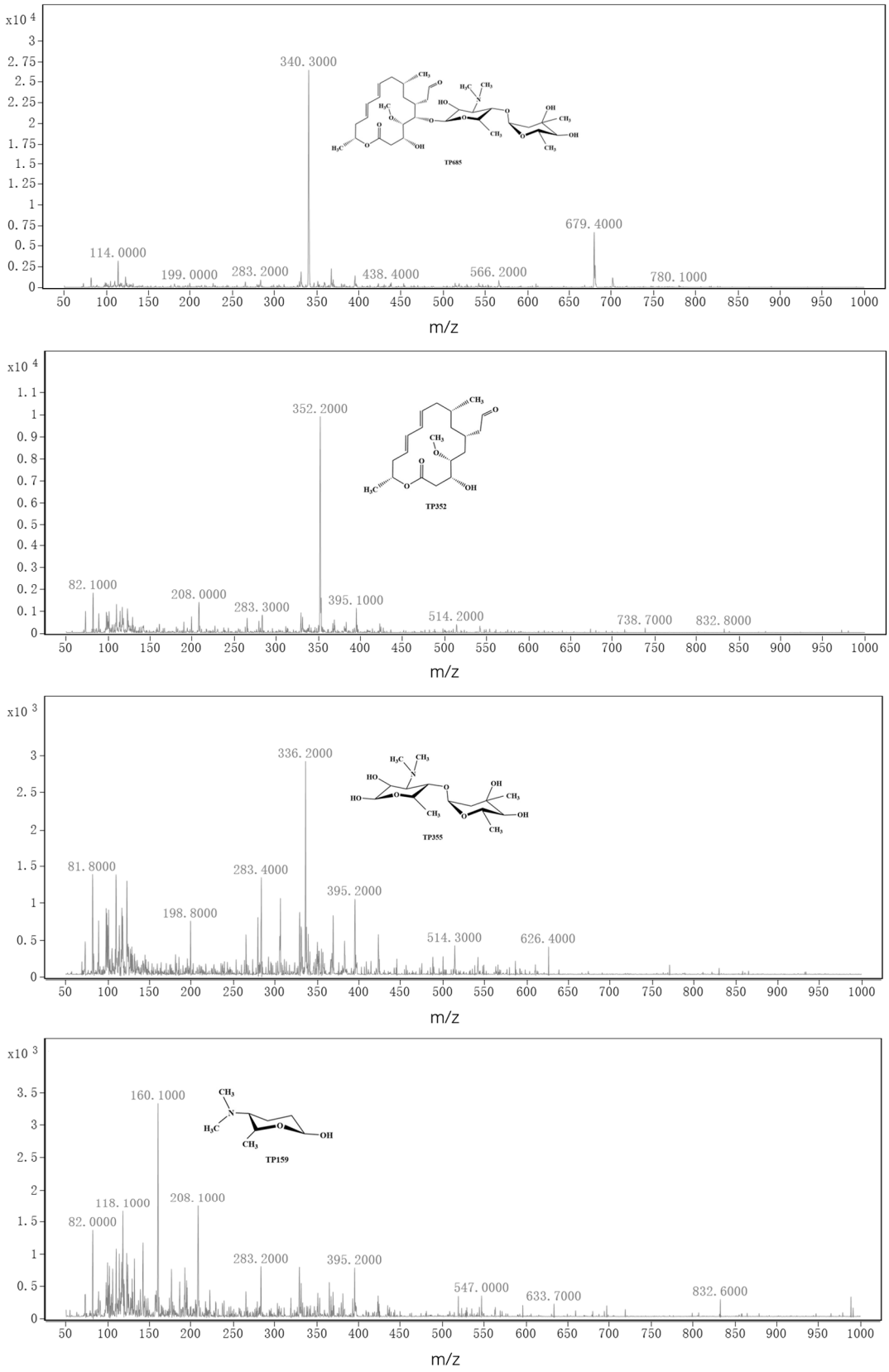

Figure S4 Mass spectra of the degradation intermediates detected using LC-MS during the degradation of SPM in the UV/Fe_3O_4/ZSM-5/Sch-H_2O_2 system.

Table S4 Retention time, chemical formula, mass charge ratio and proposed molecular structure of the detected degradation intermediates of SPM.

Compound	Retention time (min)	Chemical formula	Molecular mass (Da)	Experimental mass (m/z)	Molecular structure
SPM	8.446	$C_{43}H_{74}N_2O_{14}$	842.52	422.26	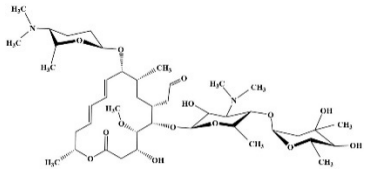
TP891	7.448	$C_{43}H_{74}N_2O_{17}$	890.50	446.27	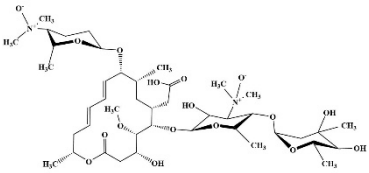
TP875	7.007	$C_{43}H_{74}N_2O_{16}$	874.52	439.26	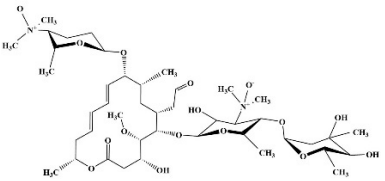
TP859-1	7.652	$C_{43}H_{74}N_2O_{15}$	858.51	430.30	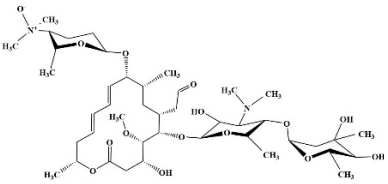
TP859-2	7.652	$C_{43}H_{74}N_2O_{15}$	858.51	430.30	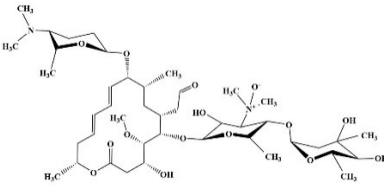
TP814	8.384	$C_{41}H_{70}N_2O_{14}$	814.48	406.17	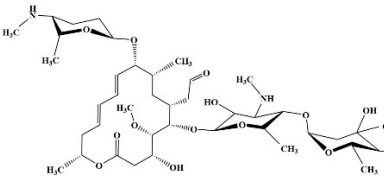
TP699	8.973	$C_{36}H_{63}N_2O_{11}$	699.20	700.39	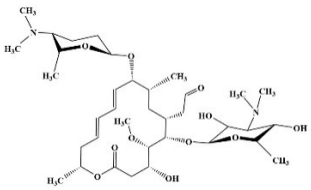

Continued Table S4

Compound	Retention time (min)	Chemical formula	Molecular mass (Da)	Experimental mass (m/z)	Molecular structure
TP685	8.093	$C_{35}H_{59}NO_{12}$	685.40	343.22	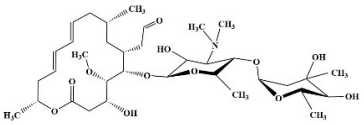
TP352	2.255	$C_{20}H_{32}O_5$	352.22	353.20	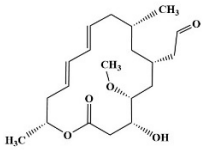
TP335	2.524	$C_{15}H_{29}NO_7$	335.19	336.20	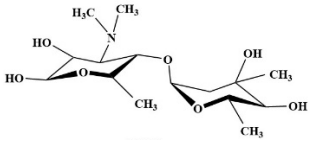
TP159	1.581	$C_8H_{17}NO_2$	159.13	160.10	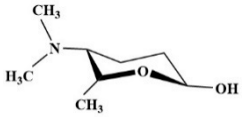

2.7 Mineralization rate

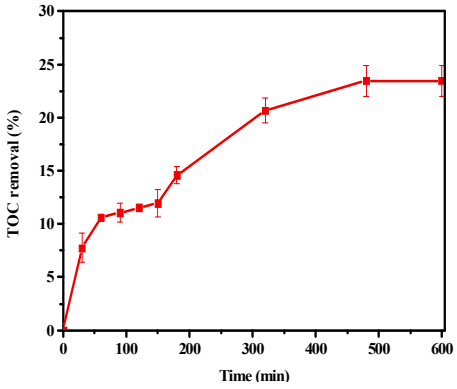

Fig.S5 Changes in TOC in the UV/Fe_3O_4/ZSM-5/Sch-H_2O_2 system.

References

1. Yan, S.; Zheng, G.; Meng, X.; Zhou, L. Assessment of catalytic activities of selected iron hydroxysulphates biosynthesized using Acidithiobacillus ferrooxidans for the degradation of phenol in heterogeneous Fenton-like reactions. *J. Separation and Purification Technology*. **2017**, 185, 83-93. http://dx.doi.org/10.1016/j.seppur.2017.05.008.